Int J Earth Sci (Geol Rundsch) (2008) 97:1045–1056
DOI 10.1007/s00531-007-0275-y

ORIGINAL PAPER

Solution-precipitation creep and fluid flow in halite: a case study of Zechstein (Z1) rocksalt from Neuhof salt mine (Germany)

Zsolt Schléder · János L. Urai · Sofie Nollet · Christoph Hilgers

Received: 19 October 2006 / Accepted: 27 October 2007 / Published online: 3 January 2008

Abstract Zechstein (Z1) rocksalt from the Fulda basin, from the immediate vicinity of the Hessen potash bed is folded into tight to isoclinal folds which are cut by an undeformed, 1 cm thick, coarse-grained halite vein. Microstructures were investigated in etched, gamma-irradiated thin sections from both the wall rock and the vein. The lack of synsedimentary dissolution structures and the widespread occurrence of plate-shaped and hopper grains in the wall-rock suggests that the sedimentary environment was perennial lake. Deformation microstructures are in good agreement with solution-precipitation creep process, and salt flow under very low differential stress. Strength contrast between anhydrite-rich and anhydrite-poor layers caused the small scale folding in the halite beds. The vein is completely sealed and composed mainly of euhedral to subhedral halite grains, which often overgrow the wall-rock grains. Those microstructures, together with the presence of occasional fluid inclusion bands, suggest that the crystals grew into a solution-filled open space. Based on considerations on the maximum value of in-situ differential stress, the dilatancy criteria, the amount of released fluids from the potash bed during metamorphism and the volume change, it is proposed that the crack was generated by hydrofracturing of the rocksalt due to the presence of the salt-metamorphic fluid at near-lithostatic pressure.

Keywords Halite · Potash salt · Deformation mechanism · Hydrofracture

Z. Schléder · J. L. Urai · S. Nollet · C. Hilgers
Geologie-Endogene Dynamik, RWTH Aachen,
Lochnerstr. 4-20, 52056 Aachen, Germany

Z. Schléder (✉)
Midland Valley Exploration Ltd,
144 West George Street,
G2 2HG Glasgow, UK
e-mail: zsolt@mve.com

Present Address:
S. Nollet
ExxonMobil Upstream Research Company,
Houston, TX, USA

Fluid transport in rocksalt

Studies of Casas and Lowenstein (1989) and Lowenstein and Spencer (1990) on Quaternary halite deposition showed that the effective porosity and permeability decrease drastically in the shallow subsurface. After about 50 m of burial the halite is nearly completely cemented, and is without any visible porosity. At depth of 100 m, the halite is tight, entirely cemented and has no measurable permeability. The very low permeability of halite is demonstrated by laboratory measurements and its ability to seal large hydrocarbon columns and fluid pressure cells. This very low permeability is maintained during halokinesis, although there are some processes which can lead to the increase in permeability.

For example, Fokker (1995) considered the long term evolution of salt permeability after abandonment of solution mining caverns. He showed that when fluid pressure in the cavern approaches lithostatic due to creep convergence, diffuse dilatancy of the roof occurs and the permeability of the salt increases to allow the slow escape of the fluid. Similar high-pressure fluid pockets (porous salt) occur also in nature and these are presumably slowly moving upwards by similar processes. This process might operate in other rock types, as suggested by the mobile hydrofracture model in Bons (2001). The detailed nature of the relation between the effective stress, differential stress and permeability was

studied in a series of experiments by Urai et al. (1986), Peach et al. (2001) and Popp et al. (2001). The authors noted that the permeability of rocksalt increases by five orders of magnitude if deformed at low temperature and mean effective stress due to microcracking and dilatancy. Similar dilatancy was reported by Wallner (1986) and Lux (2005), who noted that diffuse dilatancy occurs with dilated grain boundaries when the fluid pressure slightly exceeds σ_3 (minimum principal stress), while hydro-fracturing occurs when the fluid pressure exceeds σ_3 significantly. Natural occurrence of diffuse dilatancy was reported by Schoenherr et al. (2007) in rocksalt samples from the vicinity of oil fields in the Oman salt basin. They found oil entrapped along cleavage planes and at grain boundaries in halite and inferred that in the presence of hydrocarbons at lithostatic fluid pressure the dilatancy criterion was reached and the rocksalt became permeable for hydrocarbons and brine.

A different process leading to increased permeability of salt was reported by Lewis and Holness (1996), who measured the equilibrium water-halite dihedral angles in grain boundary triple junctions. At temperatures below 100°C these were higher than 60°, such that the small amounts of brine present in the salt are distributed in micrometer-size isolated fluid inclusions, dramatically reducing the permeability. At temperatures above 100°C and pressures of 70 MPa this value decreases below 60°, leading to a redistribution of the fluid into a thermodynamically stable network of connected, fluid filled channels at grain boundary triple junctions, dramatically increasing the permeability (comparable to that of sandstones). This process was proposed to operate in nature, at depths of about 3–4 km (cf. Schoenherr et al. 2007).

The fluids in rocksalt may be externally derived, i.e., that they can originate from below the salt succession or enter as meteoric waters from above. Alternatively, the fluids may be generated inside the salt body, by processes such as the gypsum to anhydrite conversion (if gypsum was primarily deposited) according to the following reaction:

$$CaSO_4 \cdot 2H_2O \rightarrow CaSO_4 + 2H_2O.$$

This reaction would result in a release of 40% structural water that is saturated with $CaSO_4$ (Borchert and Muir 1964). The conversion is dependent on many parameters (salinity, pore fluid pressure), and occurs between 70–105°C (Jowett et al. 1993; Warren 2006). There are some indications that this fluid may be retained in the evaporitic succession during burial, and is expelled during halokinesis (Nollet et al. 2005a). Similarly, if potash layer is intercalated, mineral transformation of the constitutive minerals (i.e., carnallite to sylvite) may also lead to a release of structural water (Borchert and Muir 1964). The process can be written as:

$$KMgCl_3 \cdot 6H_2O + 4H_2O \rightarrow KCl + Mg^{2+} + 2Cl^- + 10H_2O,$$

showing that this process needs some extra water to become active.

In shallow-water environment the halite crystals often incorporate brine inclusions due to fluctuations in growth rate (Roedder, 1984; Lowenstein and Hardie 1985; Handford 1990). The overall amount of such inclusions may make up 5% of the rocksalt (Roedder 1984). During deformation induced recrystallization of the rocksalt the fluid inclusions are swept out by the migrating grain boundary, and convert to grain boundary fluid (Schléder and Urai 2005). This fluid is then able to migrate along the grain boundaries during recrystallization of the rocksalt (Schenk and Urai 2004).

Concentration measurements of Br in rocksalt proved to be a very effective method in characterizing the primary/secondary origin of rocksalt (Kühn 1957; Fischbeck and Bornemman 1988; Siemann and Schramm 2002). Similarly, extensive studies on the fluid chemistry gave important constraints on the possible sources of fluids in rocksalt (e.g., Herrmann 1981; Herrmann and Knipping 1989; Siemann and Ellendorff 2001). Although the composition of fluids in rocksalt is well known, the processes which allows the migration of these fluids in rocksalt is still poorly understood.

In this work we present a microstructural study on a highly deformed and recrystallized Zechstein (Z1) rocksalt from Neuhof salt mine (Germany). This folded rocksalt is cut by halite veins which are completely sealed by coarse-grained halite. Based on the microstructural features we discuss the possible deformation and recrystallization mechanisms, constraints on the provenance of fluid, fluid transport processes and probable mechanism leading to vein formation.

Regional setting and samples studied

The Hessen basin, which is a southern embayment of the Permian Zechstein basin (Fig. 1), is divided into two sub-basins; the Werra and the Fulda basin (Skowronek et al. 1999; Becker 2002). Both basins are filled with an approximately 300 m tick Z1 evaporitic sequence, lying unconformably on earlier deposited Permian sediments (Figs. 2, 3). The Zechstein is composed predominantly of halite, but the sequence also includes two 1–2.5 m thick potash horizons; the Hessen and the Thüringen seams (Jahne et al. 1970). The sedimentary environment of the evaporitic sequence is predominantly shallow water (Becker 2002). The Z1 evaporites are overlain with some 350 m thick, siliciclastic Buntsandstein sediments.

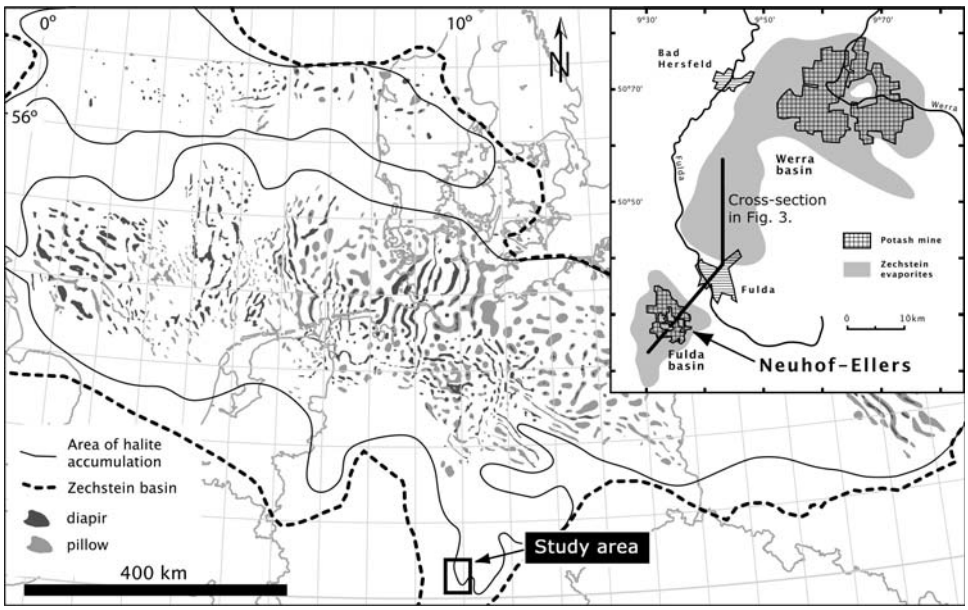

Fig. 1 The Permian Zechstein basin after Lockhorst (1998) with the location of the Werra-Fulda basins (*rectangle*). Insert detailed map of the Werra and Fulda basins (after Roth 1957)

Younger Mesozoic strata, lower Keuper, can only be found in the Fulda-graben which separates the Werra and Fulda basins (Fig. 3). It is inferred that sediments were deposited at least until the Dogger, and that the total thickness of Mesozoic sediments very likely exceeded 1,100 m (Oesterle and Lippolt 1975; Käding and Sessler 1994). The sedimentation was ceased by the end of Jurassic and was followed by erosion until the Tertiary (Leammlen 1970). The Miocene tectonic activity in the area is documented by the large accumulation of volcanic rocks on the surface (Vogelsberg, west of the Fulda basin) and by few 1–2 m thick basalt dykes which cut through the evaporite sequence (Knipping and Herrmann 1985; Käding and Sessler 1994).

The Hessen potash layer in the Fulda basin is of economic importance (Beer 1996). This potash seam is at 500 m depth (Fig. 3) and present only in the central part of the basin because a 5 km wide region is completely leached due to contact with meteoric water at the margins. In the margin zone the former potash layers now consist exclusively of a few centimeter large, clear, euhedral halite crystals (Kühn 1957; Leammlen 1970). Where not leached, the seam consists mainly of kieserite, sylvite and halite (Hartsalz) with subordinate langbeinite, kainite, rarely carnallite and some thin clay layers (Kühn 1957; Roth 1955; Leammlen 1970; Oesterle and Lippolt 1975). At the upper part of the potash seam, a 40–50 cm thick halite layer is also incorporated. Above the seam, in the lowermost part of the Upper Werra rocksalt, a 0.3–2 m thick halite layer with subordinate sylvite and carnallite can be found (Fig. 2). Although the thick halite layers are horizontal and undeformed above this halite rich layer and below the potash level, the intercalated clay and halite layers in the Hessen potash seam and the lowermost part of the Upper Werra rocksalt are occasionally extensively folded (Roth 1955; Kühn 1957; Leammlen 1970). The folds are tight to isoclinal with a near-vertical axial plane (Fig. 4). The vergence of the folds is NE and the potash layer is often sheared off from the horizontal bottom and top halite layers (Hoppe 1960). According to Leammlen (1970), the deformation was triggered by differential loading when basin became buried in the Jurassic and Cretaceous. Some authors (see Hoppe 1960) suggested that Tertiary deformation phases also played an important role in the deformation of the layers, and that the rocksalt succession deformed in a brittle manner.

In this paper we studied folded rocksalt samples from the central part of the Fulda basin from the Hessen potash layer. Samples were taken from a horizontal exploration borehole at the Neuhof-Ellers salt mine. The exploration borehole (diameter ~7 cm) was completed by the Kali und Salz GmbH with continuous coring of the complete borehole. From this core material we selected a 12 m long section, which contained intensely folded halite layers. The exact orientation of the core sample is not known, though the material represents the highly deformed Lower Werra rocksalt which was folded into the potash layer (R. Stax, pers. comm.). A detailed inspection showed that this interval contains four, approximately 1 cm thick, coarse-grained halite filled veins, from which the longest was selected for this study (Fig. 5). Based on detailed inspection of the core samples the orientation of the veins do not appear to correlate with each other and to any particular direction of the fold structures (i.e., axial plane).

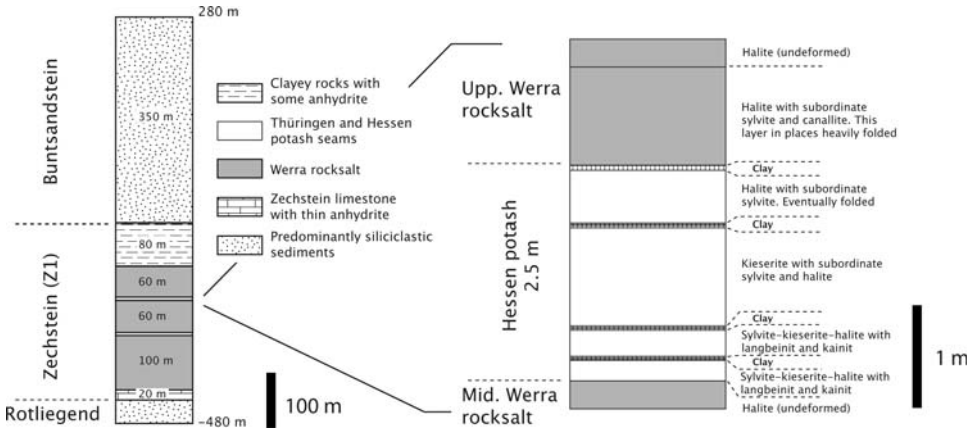

Fig. 2 Lithostratigraphic column of the Fulda basin and the Hessen potash layer after Leammlen (1970) and Käding and Sessler (1994)

Methods

Slabs were cut from the core sample, perpendicular to the vein. The slabs were then further prepared following the method described in Schléder and Urai (2005). This involved gamma-irradiation of the samples at 100°C, with a dose rate of 1–4 kGy/h to a total dose of 4 MGy, followed by thin section preparation from the slabs. The gamma-irradiation technique reveals otherwise invisible microstructures such as growth bands and subgrain boundaries (Murata and Smith 1946; Przibram 1954; Wilkins and Bird 1980; Urai et al. 1987; Schléder and Urai 2005). The sections were analyzed with transmitted and reflected light microscopy.

Observed microstructures and inferred deformation mechanisms

Wall rock

The samples consist of alteration of 0.5 mm thin layer of anhydrite/polyhalite and 5 mm thick layer of halite (Fig. 5), cut by a 1 cm thick vein which is filled with 5 mm subhedral halite grains.

The pure halite (~99%) layers consist of grains with sizes between 0.5 and 1 mm, often rich in primary fluid inclusions. The grains usually show core-mantle structures with a fluid-inclusion-rich core and a fluid-inclusion-free rim (Fig. 7b, d). In some cases the core is absent and the halite grains are completely fluid-inclusion-free (Fig. 6d). Occasionally the two neighbour grains are truncated so that their fluid-inclusion-rich parts are in contact. We interpret such core-mantle and truncated structures as they evolved with non-conservative grain boundary migration. Synsedimentary dissolution-reprecipitation process was very likely not involved in producing those structures as none of the fluid-inlcusion-rich cores show karst-like, clear halite-filled dissolution structures.

The lack of any dislocation related microstructures such as slip bands or subgrains and the presence of truncated grain cores suggest that the main deformation mechanism in this fine-grained rocksalt is solution-precipitation creep (Figs. 6, 7). Such deformation mechanism was shown to be characteristic for fine-grained wet rocksalt (Urai et al. 1986; Spiers and Schutjens 1990). During this process grains dissolve at highly stressed boundaries and after diffusion, the material crystallizes at interfaces under low normal stress (Spiers et al. 1990; Hickman and Evans 1991, Lohkämper et al. 2003).

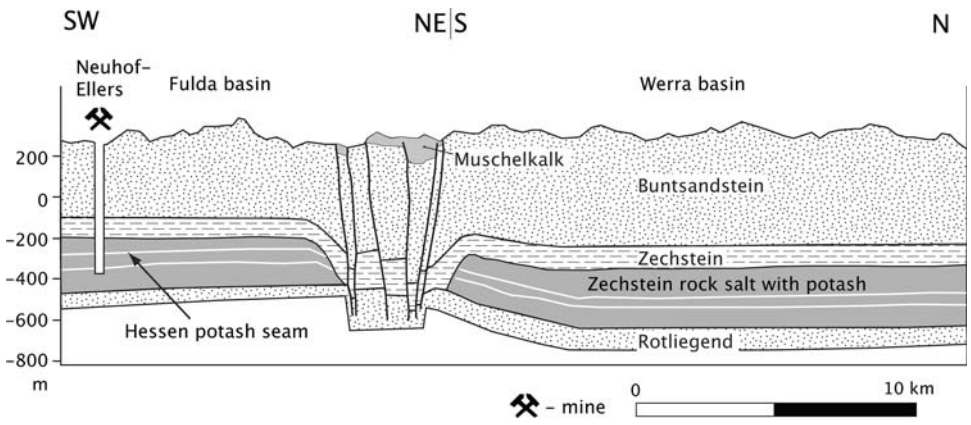

Fig. 3 Cross-section throughout the Fulda and Werra basins (after Beer 1996). The sample studied was collected in the Hessen level of Neuhof-Ellers mine. For the location of the profile see Fig. 1

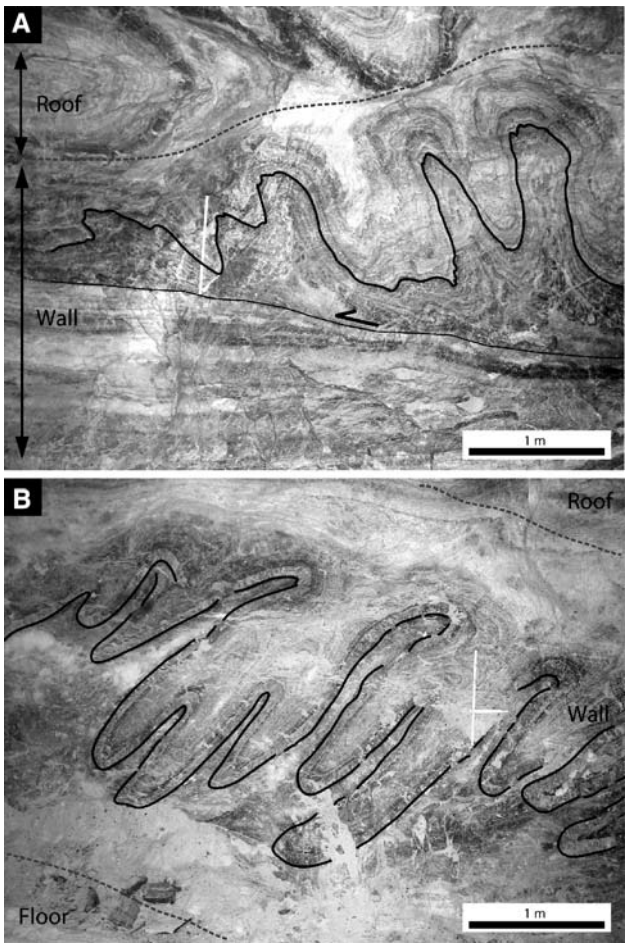

Fig. 4 The lower part of the Upper Werra Rocksalt is extensively folded in some parts of the mine. **a** Tight, isoclinal similar folds of halite and anhydrite with some reddish potash minerals. The vergence of the fold is NE. Note that the bottom layers are undeformed. **b** Isoclinal similar folds of halite and clay layers (vergence: NNE)

In this process the halite grains become elongated as compared to the intact grains and may have an aspect ratio up to two. The elongation is sub-parallel to the axial plane of the fold (Fig. 7d), suggesting that the deformation of the grains was contemporaneous with folding. An important observation is that the reprecipitated areas are fluid-inclusion-free, suggesting solution-precipitation creep during which the primary fluid inclusions were converted to grain boundary fluid. Approximately 35% of the area of the material in the halite layers is fluid-inclusion-free. Surface energy driven grain boundary migration is inferred to have played a role in the recrystallization as most of the triple junctions are close to 120°.

The anhydrite layers are often boudinaged at the limbs of the fold and show minor folds at the internal part of the hinge zone (Figs. 6a, 7a). They often contain very small, equidimensional halite grains (0.5 mm on average) which contain numerous, small (<50 μm), cubic, primary fluid inclusions. These small halite grains do not show any microstructural evidence of deformation or recrystallization except where the layers are boudinaged or folded (Fig. 6b, c). In these parts, the grains show a core-mantle structure with a fluid-inclusion-rich core and a fluid-inclusion-free rim or, alternatively, the grains may be without any core and are completely fluid-inclusion-free. The fluid-inclusion-free area in the anhydrite rich layers makes up 5% of the halite.

This difference in extent of the deformation in the anhydrite rich and anhydrite poor layers can be explained by the higher mechanical strength of the anhydrite-rich layer causing strain concentration in the halite-rich layers (Bons 1993). This difference in rheology might also be accounted for the strong folding of the rocksalt layers.

The microstructures show that primary subaqueous depositional structures are well preserved. The halite layers are composed exclusively of cumulates of mm sized plates, cubes and hoppers (Fig. 7b, d) and were very likely crystallized at the brine-air interface originally (Warren 2006). The lack of a syndepositional dissolution surface implies that the halite was precipitated in a perennial halite-saturated brine (Lowenstein and Hardie 1985). The thin anhydrite layers might have precipitated originally as gypsum when the brine body was cyclically diluted with halite-unsaturated water but was converted later to

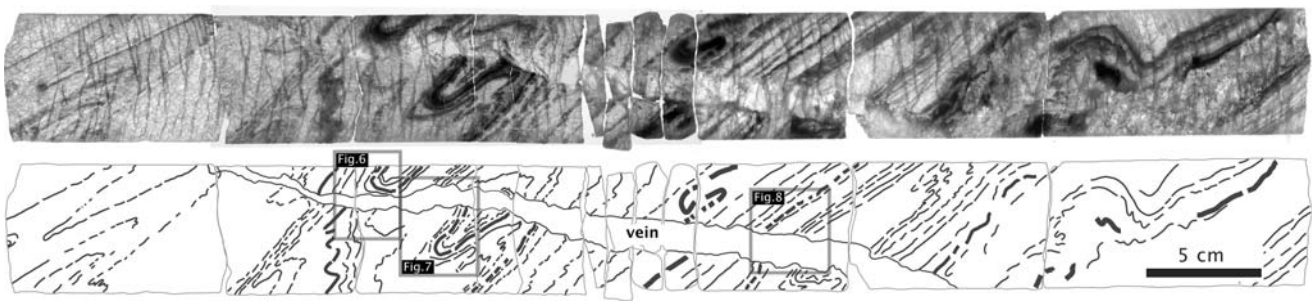

Fig. 5 Scanned image of the studied core interval together with the hand-drawing of traced anhydrite layers (*black lines*). The transparent layer which cut through the folded layers is a coarse-grained, halite-filled vein. Note that there is a slight offset in the wall-rock across the vein. The locations of the studied thin sections are indicated with *rectangles*

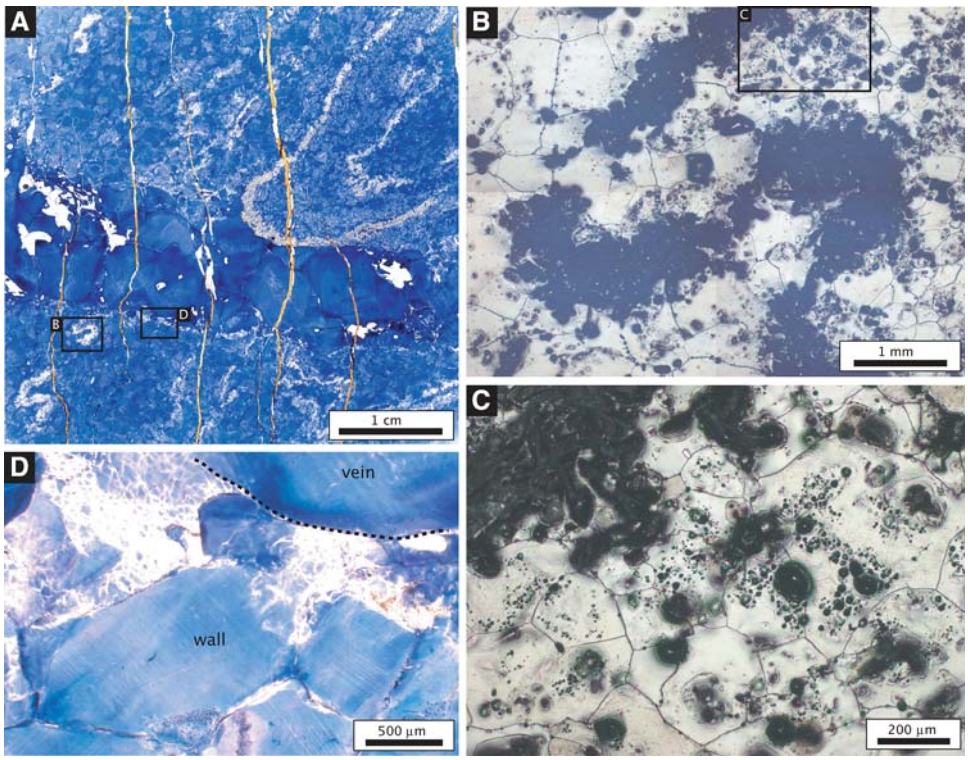

Fig. 6 **a** Overview image of the gamma-irradiated thin section. For the location see Fig. 5. White anhydrite bands are isoclinally folded. The E-W trending coarse-grained part is the vein. **b** Detail of the folded anhydrite layer in reflected light. For the location see image **a**. Note that the anhydrite layers are boudinaged and that the halite grains are free of substructures. **c** Detail of image **b**. The *black dots* inside the halite grains are primary fluid inclusions opened up during sample preparation. Note again that the halite is without any substructure. **d** Detail of the vein-wall interface photographed in transmitted light (for location see image **a**). The grain boundaries occur as *dark lines*, the subgrains as *white polygons*. Note that at the presence of subgrains is limited to a narrow zone at the vein-wall interface

anhydrite during burial (Shearman 1970). The timing of this mineral transformation is not entirely clear.

Halite grains close to the vein occasionally contain well-developed, equidimensional subgrains. The thickness of such subgrain-rich zone does not exceed a few millimeters (Fig. 6d). The presence of these subgrains is interpreted to relate to the brittle process during cracking of the rocksalt.

Based on the microstructures, it is inferred that the operating deformation mechanism during folding is solution-precipitation creep. The rheology of halite deforming by this process can be described by the following flow law of Spiers et al. (1990):

$$\dot{\varepsilon} = 4.7 \times 10^{-4} \exp\left(-24530/RT\right)(\sigma_1 - \sigma_3)/TD^3$$

for which the strain rate $(\dot{\varepsilon})$ is in s^{-1}, the pre-exponential constant is in K mm^3 MPa^{-1} s^{-1}, apparent activation energy is in J mol^{-1}, Boltzmann's gas constant (R) is in J mol^{-1} K^{-1}, temperature (T) is in K, differential stress (σ_1–σ_3) is in MPa and grain size (D) is in mm. For the calculations, we assumed that the deformation temperature was around 80°C. This assumption is based on works of Oesterle and Lippolt (1975) and Werner and Doebl (1974) who considered the required temperature for metamorphosis of potash minerals and formation of langbeinite and suggested that the deepest burial exceeded 1 km and that the geothermal gradient was extremely high (1°C/16 m). Rheological considerations are based on the absence of dislocation creep processes, and indicate that this fine-grained salt is very weak, i.e., deforms at $\dot{\varepsilon} \sim 5 \times 10^{-10}$ s^{-1} (T = 353 K and D = 0.5 mm) at low differential stresses (σ_1–σ_3 = 0.1–0.3 MPa). This is an upper bound estimate, as for in-situ differential stress higher than this dislocation and grain boundary migration microstructures would have developed (Urai et al. 1986).

Vein

The vein is mainly filled with large halite crystals (5 mm) and with a few percent of anhydrite (Figs. 6, 7, 8). The halite grains are euhedral and the gamma-irradiated sections show growth banding with alteration of dark-blue coloured and pale-blue coloured layers. The orientation of the growth bands is crystallographically controlled and parallel to {100} facets (Figs. 8b–d). In some crystals, fluid inclusions arranged parallel to the growth banding are observed implying that the growth occurred in the presence of fluids. No subgrains were observed in the halite grains, except some elongated ones, which are perpendicular to the grain boundaries (Fig. 8c). These subgrains are very similar to those observed by Nollet et al. (2005a) and are interpreted as they were synkinematically grown-in with the growth of the crystal. Such edgewise propagation of subgrain boundaries behind migrating grain boundaries was reported by Means and Ree (1988) in experimentally deformed octachloropropane. Equidimensional subgrains or lobate grain boundaries were not observed in the vein, suggesting that the grains are undeformed, which in turn

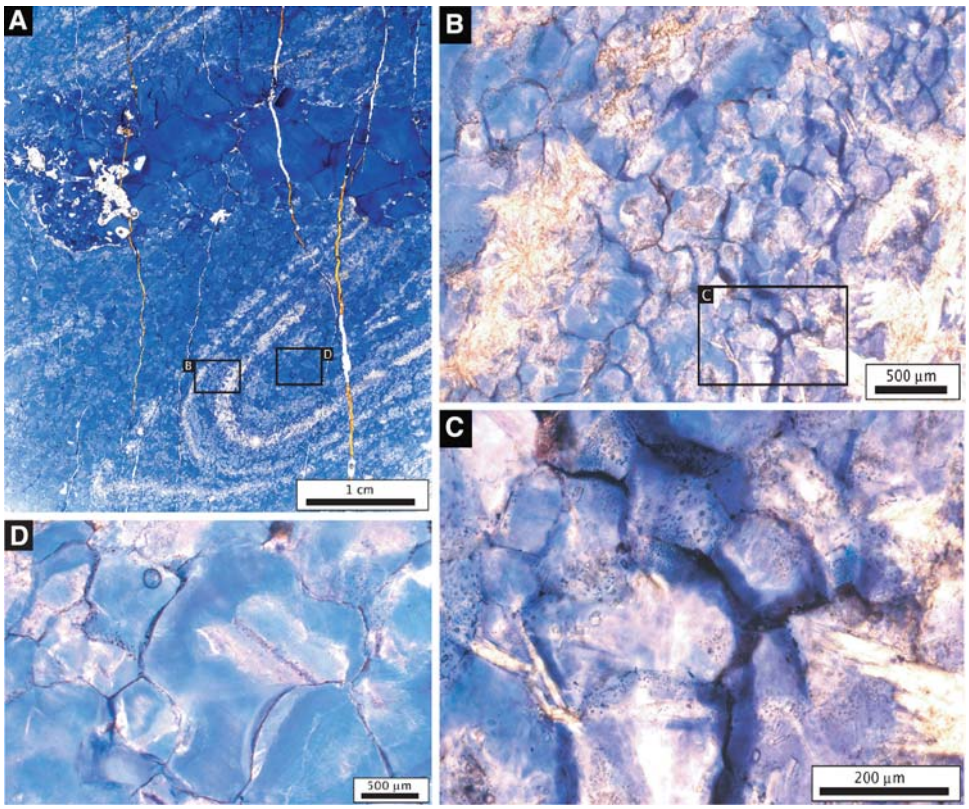

Fig. 7 **a** Overview image of the gamma-irradiated thin section. The thin anhydrite layers (*white*) outline a tight, isoclinal fold. Note that the E-W trending vein contains also subordinate amount of anhydrite (occur as *white patches*). The N-S oriented cracks were presumably introduced during the drilling and are now filled with resin. The locations of detail images of *b* and *d* are indicated with *rectangles*. **b** Detail of image **a** shows a halite layer between two anhydrite bands in transmitted light. The off-white parts inside the halite grains are fluid-inclusion-rich zones. The fluid-inclusion-free zones are interpreted as they formed during deformation when the moving grain boundaries swept out the inclusions from the grains. Note that the fluid-inclusion-free parts are favorably oriented sub-parallel to the axial plane of the fold. **c** Detail of image **b** shows a recrytsallized zone (*dark coloured*) which is sub-parallel to the axial plane. **d** Detail of image **a** in transmitted light. Grain boundaries occur as *dark lines*. The grain in the middle contains an elongated fluid-inclusion-rich plate. Such a plate is interpreted as nucleated at the brine-air interface, after which it sank to the bottom. The plate is surrounded with fluid-inclusion-free rim, which is interpreted as recrystallized part

implies that the vein postdates the folding of the halite layers.

Similar blocky veins to those described here were widely observed for example in shale, sandstone and limestone (Mügge 1928, Durney and Ramsay 1973, Fisher and Brantley 1992, Bons and Jessell 1997; Hilgers 2000; Nollet 2005). Numerical simulations of crystal growth in fractures have shown that such veins form when the opening velocity of the fractures is larger than the growth velocity of the crystals (Hilgers et al. 2001; Nollet et al. 2005). This indicates that the formation of such veins require relatively wide, open gaps, which stay open as long as they become sealed with crystals growing in the gap.

The crystals in the vein may either grow by epitaxial overgrowth of the wall-rock grains or after nucleation of new crystals in the oversaturated fluid in the gap (e.g., Bons and Jessell 1997). In the case when the crystals overgrow the wall-rock grains, growth competition takes place based on differences in the crystallographic orientation, resulting in a microstructure with a crystallographic preferred orientation (Nollet et al. 2005). In the vein studied here, some vein-filling halite crystals are clearly the result of epitaxial overgrowth on wall-rock halite grains, although some do not have a connection to the wall-rock, and are completely enclosed with other crystals (Fig. 5a). This apparent feature may well be due to sectioning effect. The crystals, which are overgrowth of wall-rock grains, have a profound cornet-inward orientation (Fig. 5c), most probably reflecting growth competition (Thijssen 1995; van Suchtelen 1995).

Discussion

The presence of subgrains along the vein wall interface can be explained by the fracturing process of the salt. The

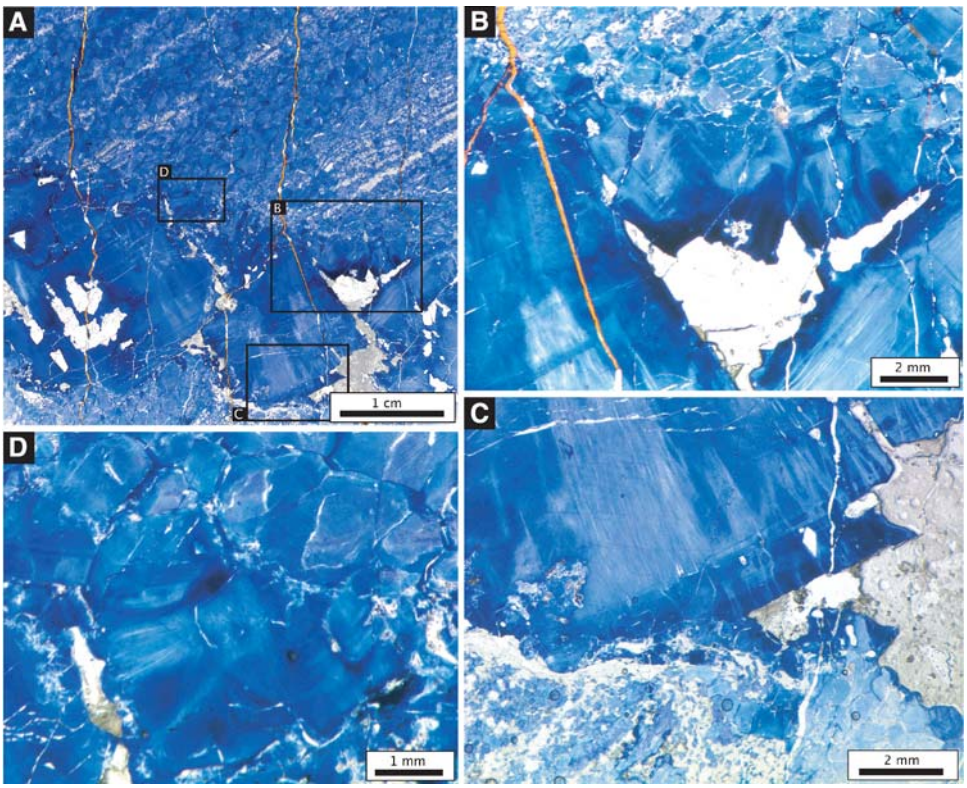

Fig. 8 **a** Overview image of the gamma-irradiated thin section. The E-W trending vein is filled with large, euhedral halite grains. Anhydrite and potash mineral is also intercalated (show up as *white patches*). The places of detail images of *b*, *c* and *d* are indicated with *rectangles*. **b** Detail of the wall-vein interface. Note that the vein crystals overgrow the wall rock grains. The N-S oriented cracks are due to drilling and sample preparation. The white material patch indicates the former place of the potash, which has been dissolved during sample preparation. **c** Detail of the contact of the coarse grained vein halite and the wall rock. The elongated *white lines* are grown-in subgrains. Note the growth bands which are parallel to the {100} crystal facets. At the right side, the *white patch* shows the former place of the intercalated potash. **d** Image illustrating the vein-wall interface. Note that the vein crystals overgrow the wall-rock grains

presence of primary fluid inclusions along some of the crystal facets and the absence of deformation in the vein halite implies growth in a static environment and no deformation after the vein was sealed, because this would have formed subgrains in the large vein crystals.

Different mechanisms may provide space for vein formation. It is known from the literature that in ephemeral sedimentary environment the rocksalt often contains desiccation cracks, which are later filled with halite during synsedimentary processes. The presence of the studied vein can not be explained with such a mechanism as the vein cross cuts isoclinally folded rocksalt.

Hoppe (1960) suggested that the rocksalt deformed in a brittle manner during the late Tertiary tectonic uplift of the area and implied that the veins might be associated to those deformations. However, this paper did not provide a mechanical explanation of the process and extensive work on salt mechanics shows that dilatant fracturing of rocksalt at depth and high effective stresses is not possible.

We propose that these veins were generated by hydrofracturing. Conditions for hydrofracturing of rocksalt were studied by Fokker (1995), Popp et al. (2001) and Lux (2005) using laboratory experiments, defining the boundaries of the dilatancy field as a function of effective mean stress and differential stress. To reach dilatancy at the very low in-situ differential stress at the Hessen layer, the in-situ effective stress had to be very low to enter to the dilatancy field (Fig. 9), and this in turn implies fluid pressures very close to the overburden stress. The fluid pressure had to exceed the minimum stress sufficiently to open a fracture and not increase porosity by diffuse dilatancy.

To cause hydrofracturing of the rocksalt, large amount of highly overpressured fluid is needed. In what follows, we further discuss whether this mechanism is an alternative explanation for the vein generation in the rocksalt.

Open cracks containing high pressured fluid or gas have been reported in several potash mines (Baumert 1928; Weiss 1980). Borchert and Muir (1964) noted asymptotic decrease of flow rate of fluids with time from such cracks in potash mines and suggested that the cracks are not penetrative and are not in contact with meteoric waters.

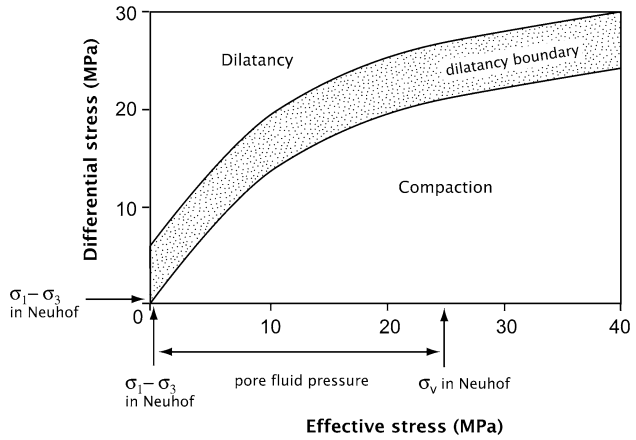

Fig. 9 Graph shows the compaction and the dilatant field for rocksalt (after Popp et al. 2001). We consider the hydrofracturing as one possible mechanism for the formation of the veins in the Hessen layer. To reach dilatancy at the very low in-situ differential stress at the Hessen layer, the in-situ effective stress had to be very low. This was probably attained by the presence of high-pressured fluid resulted from mineral transformations

Fluid sources

The origin of potash minerals is an unsolved problem in many potash deposits worldwide (Warren 2006). It is generally agreed that a paragenesis of sylvite, kieserite and halite is not a primary precipitate, since it would require sea temperature above 72°C. This suggests that these are results of subsequent transformation of some pre-existing primary potash minerals (Kühn 1957; Warren 2006). Gottesmann (1963) found microstructural evidence for the transition of primary carnallite to sylvite in the Stassfurt potash seam, and suggested that such metamorphism of carnallite is a common mechanism in the potash beds. Observations on recent potash precipitates also suggest that the carnallite is the main potash phase (Warren 2006). On the contrary, based on mutual relationship between halite and sylvite, Lowenstein and Spencer (1990) argued that sylvite rather than carnallite was the primary precipitate in the Rhine Graben (Germany), Salado formation (New Mexico, USA) and Prairie formation (Saskatchewan, Canada). Borchert and Muir (1964, p 172) suggested that the secondary sylvite might convert back to carnallite when in contact with $MgCl_2$ rich brines, making the differentiation between primary and secondary potash minerals very difficult. According to Baar (1959) the carnallite conversion to sylvite involves a volume decrease.

The origin of the potash layers in the Werra and Fulda basins is also not entirely clear (Käding and Sessler 1994). Roth (1955) suggested a metamorphic origin for the langbenite in the Hessen layer by metamorphosis of sylvite and kieserite in the presence of NaCl containing solution according to: $2KCl + 3MgSO_4{\cdot}H_2O \rightarrow K_2SO_4{\cdot}2MgSO_4 + MgCl_2 + 3H_2O$. Oesterle and Lippolt (1975) determined the age of the langbeinite crystals using K/Ar and Rb/Sr radiometric methods and found that the langbeinite was formed at 150 Ma ago. They argued that the langbeinite formation coincided with the deepest burial (>1,100 m) and main folding went of the salt layers. They suggested that the geothermal gradient was high, and that the temperature of 83°C was reached at that depth (>1,100 m, Werner and Doebl 1974). In their model, Cenozoic tectonics and the Miocene volcanism do not have a significant effect on the salt succession. Kühn (1957) suggested that the kainite is also a metamorphic mineral and a result of the reaction of sylvite and kieserite ($KCl + MgSO_4{\cdot}H_2O + 2H_2O \rightarrow KCl{\cdot}MgSO_4{\cdot}3H_2O$). He noted that the kainite generation would accompany a volume increase of 28%.

As all the above cited studies suggest that the Hessen layer underwent significant metamorphism, it seems viable to assume that the sylvite in the Hessen layer was once carnallite and the following reaction occurred: $KMgCl_3{\cdot}6H_2O + 4H_2O \rightarrow KCl + Mg^{2+} + 2Cl^- + 10H_2O$. Thus if we consider that the layer contains of about 20% of sylvite (Roth 1955) and that this sylvite was originally carnallite, the conversion results in release of 1.4 m^3 of water per 1 m^3 of admixture of halite, kieserite and carnallite. It has to be noted here that presence of the water, which results in the breakdown of the carnallite, is not entirely clear. It may have been generated by the dehydration of clay, gypsum-anhydrite conversion in the rocksalt layers or intergranular water resulting from recrystallization of rocksalt.

Mineral transformation also occurred in the anhydrite layers. Since the $CaSO_4$ precipitates primarily as gypsum rather than anhydrite (Warren 2006 and references therein), it is supposed that the ~8 m thick anhydrite bed at the bottom and the top of the Z1 sequence was once a gypsum layer which later converted to anhydrite. During conversion, according to the equation $CaSO_4{\cdot}2H_2O \rightarrow CaSO_4 + 2H_2O$, it is calculated that 1 m^3 gypsum results in 0.62 m^3 of anhydrite and 0.48 m^3 of $CaSO_4$ rich water (Borchert and Muir 1964, p 133). It is very likely that the water, released from this mineral conversion, did not play a significant role in the metamorphic processes in the Hessen layer, because there is some 150 m thick rocksalt between the anhydrite and potash layers, through which this amount of fluid had to migrate. The conversion of the thin gypsum layers (now anhydrite) observed in the samples also did not lead to the release of significant amount of fluids, as suggested by the thickness of those layers (~0.5 mm).

Another possible fluid source is the expulsion of primary fluid inclusions during recrystallization of rocksalt.

According to measurements on the samples in reflected light, the area occupied by fluid inclusions in the fluid-inclusion-rich core is about 4%. Assuming that the fluid-inclusions occurred evenly distributed over the halite grain before recrystallization, we take this value as representative water content for the undeformed state. Based on a combination of transmitted and reflected light images of gamma-irradiated sections, we measured that the recrystallized part of the grains is about 30%. Thus, the calculated amount of water which is released during recrystallization is 0.012 m^3 per 1 m^3 of deformed halite. The amount of this fluid, similarly to that produced by the transformation of gypsum to anhydrite in the samples, is very small. Some water is also expelled from the clay layers during their compaction, though the amount of these fluids is also negligible.

Considering all the possibilities for fluid sources, the largest source of water is that from the potash bed during the conversion of potash minerals. This metamorphic fluid is generated at pressures very close to the overburden stress, and is able to create hydrofractures in the overlying rocksalt (Fig. 9).

Precipitation of halite in the vein

Detailed calculations on the required amount of fluids from which the halite precipitated as well as consideration of all the processes leading to the complete sealing of the vein is beyond of the scope of this paper. Once the crack opens, there are different possibilities for generation of supersaturation of the fluid and precipitation of halite from the solution, for example drop in temperature, in pressure or mixing of solutions with different composition. Temperature or pressure drop requires very large amount of fluids to completely seal a vein so that it is very unlikely that they played an important role in halite precipitation (Adams 1931; Herrmann and Knipping 1989). Mixing of solutions with different chemical compositions can precipitate the maximum amount of halite. Herrmann and Knipping (1989) consider mixing of $MgCl_2$ and NaCl solutions, and calculate that 12.2 m^3 NaCl solution and 13 m^3 $MgCl_2$ solution is required to seal completely a 1 cm thick 10 m × 10 m tabular shaped fracture. After the complete sealing, the amount of the rest solution is 23.4 m^3. Based on Br concentration measurements in a halite-filled vein, Fischbeck and Bornemman (1988) suggest this process as the most plausible explanation for the sealing of halite veins. It has to be noted here that while the $MgCl_2$-rich solution can be easily explained by metamorphic reactions in the potash layer, the source of the required amount of NaCl solution is not clear.

Conclusion

In this study we analyzed a folded rocksalt sample with a coarse-grained, halite-filled vein from the vicinity of the Hessen potash layer (Fulda basin). The aim was to characterize the deformation mechanism in the rocksalt and to constrain the processes which led to the vein formation based on the microstructures. We conclude the following:

- The depositional environment for the rocksalt is perennial lake. The salt crystals nucleated at the brine-air interface and then sunk to the bottom of the lake. The anhydrite layers were presumably precipitated as gypsum and are due to cyclic arrival of halite-unsaturated water.
- Due to the synsedimentary processes, the rocksalt sample is fine-grained, so that it is very weak and deforms entirely with solution-precipitation processes. Strength variations in anhydrite-rich and poor layers are accounted for the strong folding in the halite beds.
- The Zechstein evaporite contains undeformed euhedral halite veins. The vein-wall interface shows a zone of subgrains, indicating strain localization due to fracturing. The vein microstructure (subhedral grains) suggests that they grew freely into an open space.
- The potash mineral transformations result in the release of large amount of fluids. This metamorphic fluid is generated at pressures very close to the overburden stress, and is able to create hydrofractures in the overlying rocksalt.

Acknowledgments The authors thank R. Stax (K+S Salz GmbH) for providing the samples and M. Thomé (Forschungszentrum Jülich) for carrying out the gamma-irradiation. Reviews of P.D. Bons and Y. Maystrenko improved the manuscript. This work was performed as part project of SPP 1135 (project UR 64/5-1-2) financed by the Deutsche Forschungsgemeinschaft.

References

Adams LH (1931) Equilibrium in binary systems under pressure. I. An experimental and thermodynamic investigation of the system NaCl-H_2O at 25°C. J Am Chem Soc 53:3769–3813

Baar CA (1959) Über gleichartige Gebirgsverformungen durch bergmännischen Abbau von Kaliflözen bzw. durch chemische Umbildung von Kaliflözen in geologischer Vergangenheit. Freiberger Forsch.-H, pp 137–159

Baumert B (1928) Über Laugen- und Wasserzuflüsse im Deutschen Kalibergbau, RWTH Aachen

Becker F (2002) Zechsteinkalk und Unterer Werra-Anhydrit (Zechstein 1) in Hessen: Fazies, Sequenz-stratigraphie und Diagenese. Geologische Abhandlungen Hessen 109:1–231

Beer WW (1996) Kalilagerstätten in Deutschland. Kali und Steinsalz 12(Heft 1):18–30

Bons P (1993) Experimental deformation of polyphase rock analogues. Unpublished PhD thesis, University of Utrecht, Utrecht

Bons P (2001) The formation of large quartz veins by rapid ascent of fluids in mobile hydrofractures. Tectonophysics 336:1–17

Bons P, Jessell MW (1997) Experimental simulation of the formation of fibrous veins by localised dissolution-precipitation creep. Mineral Mag 61:53–63

Borchert H, Muir RO (1964) Salt deposits. The origin, metamorphism and deformation of evaporites. D. van Nostrand Company Ltd., London, p 338

Casas E, Lowenstein TK (1989) Diagenesis of saline pan halite: comparison of petrographic features of modern, Quaternary and Permian halites. Sediment Petrol 59(5):724–739

Durney DW, Ramsay JG (1973) Incremental strains measured by syntectonic crystal growths. In: De Jong KA, Scholten R (eds) Gravity and tectonics. Wiley, New York, pp 67–96

Fischbeck R, Bornemman O (1988) Genetische Überlegungen aufgrund von Brom-Bestimmungen an halitischen Kluftfüllungen is Salzgesteinen des Salzstocks Gorleben, Niedersachsen. Fortschritte der Mineralogie 66(1):35

Fisher DM, Brantley SL (1992) Models of quartz overgrowth and vein formation: deformation and episodic fluid flow in an ancient subduction zone. J Geophys Res 97:20043–20061

Fokker PA (1995) The behaviour of salt and salt caverns. Unpublished PhD thesis, TU Delft, Delft

Gottesmann W (1963) Eine häufig auftretende Struktur des Halits im Kaliflöz, Stassfurt. Geologie 12(5):576–581

Handford RC (1990) Halite depositional facies in a solar salt pond: a key to interpreting physical energy and water depth in ancient deposits? Geology 18:691–694

Herrmann AG (1981) Grundkenntnisse über die Entstehung mariner Salzlagerstätten. Der Aufschluss—Zeitschrift für Freunde der Mineralogie und Geologie Jh. 32(Feb 1981):1–72

Herrmann AG, Knipping B (1989) Stoffbestand von Salzstöcken und Langzeitsicherheit für Endlager radioaktiver Abfälle. PTB informiert: Fachbeiträge zur Sicherstellung und zur Endlagerung radioaktiver Abfälle 1(89):2–50

Hickman SH, Evans B (1991) Experimental pressure solution in halite; the effect of grain/interphase boundary structure. J Geol Soc Lond 148:549–560

Hilgers C (2000) Vein growth in fractures—experimental, numerical and real rock studies. Unpublished PhD thesis, RWTH Aachen, Aachen

Hilgers C, Koehn D, Bons P, Urai JL (2001) Development of crystal morphology during unitaxial growth in a progressively widening vein: II. Numerical simulations of the evolution of antitaxial fibrous veins. J Struct Geol 23:873–885

Hoppe W (1960) Die Kali- und Stensalzlagerstätten des Zechsteins in der Deutschen Demokratischen Republik. Teil 1: Das Werra-Gebiet. Freiberger Forsch.-H. C 97(I):166

Jahne H, Oettel S, Voitel R (1970) Die feinstratigrapische Gliederung des Salinars im Zechstein 1 des Werra-Kaligebietes. Ber deutsch Ges geol Wiss A Geol Paläont 15(4):505–515

Jowett EC, Cathles LM, Davis BW (1993) Predicting depths of gypsum dehydration in evaporitic sedimentary basins. Am Assoc Pet Geol Bull 77(3):402–413

Knipping B, Herrmann AG (1985) Mineralreaktionen und Stofftransporte an einem Kontakt Basalt-Carnallitit in Kalisalzhorizont Thüringen der Werra-Series des Zechsteins. Kali un Steinsalz 9:111–124

Käding KC, Sessler W (1994) Befahrung Kalibergwerkes Neuhof-Ellers der Kali und Steinsaz AG bei Fulda (Exkursion G am 8. April 1994). Jber Mitt oberrhein geol Ver 76:191–197

Kühn R (1957) Führung durch das Kalibergwerk Neuhof-Ellers, obere Sohle, nebst einigen Beiträgen zur Petrographie des Werra-Fulda-Kalireviers. Fortschritte der Mineralogie 35:60–120

Leammlen M (1970) Geologische Karte von Hessen 1:25000 mit Erläuterungen. Blatt Nr. 5523 Neuhof, Wiesbaden, Germany,

Lewis S, Holness M (1996) Equuilibrium halite-H2O dihedral angles: high rock-salt permeability in the shallow crust? Geology 24(5):431–434

Lockhorst A (ed) (1998) NW European gas atlas-composition and isotope ratios of natural gases. GIS application on CD-ROM by the British Geological Survey, Bundesanstalt für Geowissenschaften und Rohstoffe, Danmarks og Gronlands Geologiske, Undersogelse, Netherlands Instituut voor Toegepaste geowetenschappen, Panstwowy Instytut Geologiczny, European Union

Lohkämper THK, Jordan G, Costamagna R, Stöckhert B, Schmahl WW (2003) Phase shift interference microscope study of dissolution-precipitation processes of nonhydrostatically stressed halite crystals in solution. Contrib Mineral Petrol 146(3):263–274

Lowenstein TK, Hardie LA (1985) Criteria for the recognition of salt-pan evaporites. Sedimentology 32:627–644

Lowenstein TK, Spencer RJ (1990) Syndepositional origin of potash evaporites: petrographic and fluid inlcusion evidence. Am J Science 290:1–42

Lux K-H (2005) Long-term behaviour of sealed liquid-filled salt cavities—a new approach for physical modelling and numerical simulation—basics from theory and lab investigations. Erdöl Erdgas Kohle 121:414–422

Means WD, Ree JH (1988) Seven types of subgrain boundaries in octachloropropane. J Struct Geol 10:765–770

Murata KJ, Smith RL (1946) Manganese and lead coactivators of red fluorescence in halite. Am Mineral 31:527–538

Mügge O (1928) Über die Entstehung faseriger Minerale und ihrer Aggregationsformen. Neues Jahrbuch für Mineralogie, Geologie und Paläontologie 58A:303–348

Nollet S (2005) Fracture sealing processes in sedimentary basins—a multi-scale approach. Unpublished PhD thesis, RWTH Aachen, Aachen

Nollet S, Hilgers C, Urai J (2005a) Sealing of fluid pathways in overpressure cells—a case study from the Buntsandstein in the Lower Saxony Basin (NW Germany). Int J Earth Sci 94(5–6):1039–1056

Nollet S, Urai JL, Bons PD, Hilgers C (2005b) Numerical simulations of polycrystal growth in veins. J Struct Geol 27(2):217–230

Oesterle FP, Lippolt HJ (1975) Isotopische datierung der Langbeinitbildung in der Kalisalzlagerstätte des Fuldabeckens. Kali und Steinsalz 6:391–398

Peach CJ, Spiers CJ, Trimby PW (2001) Effect of confining pressure on dilatation, recrystallization, and flow of rock salt at 150°C. J Geophys Res 106(B7):13315–13328

Popp T, Kern H, Schulze O (2001) Evolution of dilatancy and permeability in rock salt during hydrostatic compaction and triaxial deformation. J Geophys Res 106(B3):4061–4078

Przibram K (1954) Irradiation colours in minerals. Endeavour 13(49):37–41

Roedder E (1984) The fluids in salt. Am Mineral 69:413–439

Roth H (1955) Ausbildung und Lagerungsformen des Kaliflöz "Hessen" im Fuldagebiet. Z deutsch geol Ges 105(4):674–684

Roth H (1957) Befahrung des Kalisalzbergwerkes "Wintershall" der Gewerkscahft Wintershall in Heringen/Werra. Fortschr Miner 35(1):82–88

Schenk O, Urai JL (2004) Microstructural evolution and grain boundary structure during static recrystallization in synthetic polycrystals of sodium chloride containing saturated brine. Contrib Mineral Petrol 146:671–682

Schléder Z, Urai JL (2005) Microstructural evolution of deformation-modified primary halite from the Middle Triassic Röt Formation at Hengelo, The Netherlands. Int J Earth Sci 94:941–955

Schoenherr J, Janos L, Urai, Peter A. Kukla, Ralf Littke, Zsolt Schléder, Jean-Michel Larroque, Mark J. Newall, Nadia Al-Abry, Hisham A. Al-Siyabi, Zuwena Rawahi (2007) Limits to

the sealing capacity of halite: a case study of the Infra-Cambrian Ara Salt from the South Oman Salt Basin. AAPG Bull 91(11):1541–1557

Shearman DJ (1970) Recent halite rock, Baja California, Mexico. Transaction of Mining and Metall 79B:155–162

Siemann MG, Ellendorff B (2001) The composition of gases in fluid inclusions of late Permian (Zechstein) marine evaporites in Northern Germany. Chem Geol 173(1–3):31–44

Siemann MG, Schramm M (2002) Henry's and non-Henry's law behavior of Br in simple marine systems. Geochim Cosmochim Acta 66(8):1387–1399

Skowronek F, Fritsche J-G, Aragon U, Rambow D (1999) Die Versenkung und Ausbreitung von Salzabwasser im Untergrund des Werra-Kaligebiets. Geologische Abhandlungen Hessen 105:1–83

Spiers CJ, Schutjens P (1990) Densification of crystalline aggregates by fluid phase diffusional creep. In: Barber DJ, Meredith PD (eds) Deformation processes in minerals, ceramics and rocks. Unwin Hyman, pp 334–353

Spiers CJ, Schutjens PMTM, Brzesowsky RH, Peach CJ, Liezenberg JL, Zwart HJ (1990) Experimental determination of constitutive parameters governing creep of rocksalt by pressure solution. In: Knipe RJ, Rutter EH (Eds) Deformation mechanisms, rheology and tectonics geological society of London special publication, vol. 54, pp. 215–227

Thijssen JM (1995) Simulation of polycrystalline growth in 2 + 1 dimensions. Phys Rev Lett 51:1985–1988

Urai JL, Spiers CJ, Zwart HJ, Lister GS (1986) Weakening of rock salt by water during long-term creep. Nature (London) 324(6097):554–557

Urai JL, Spiers CJ, Peach C, Franssen RCMW, Liezenberg JL (1987) Deformation mechanisms operating in naturally deformed halite rocks as deduced from microstructural investigations. Geologie en Mijnbouw 66:165–176

van Suchtelen J (1995) The geometry of crystal growth. In: Sunagawa I (Ed) Morphology of crystals. Kluwer, Dordrecht, p 419

Wallner M (1986) Frac-pressure risk in rock salt. In: SMRI Autumn Meeting, Amsterdam, The Netherlands, 21–24 September, pp 1–14

Warren J (2006) Evaporites: sediments, resources and hydrocarbons. Springer, Heidelberg, p 1036

Weiss MH (1980) Möglichkeiten der entstehung sowie art, umfang und Tektonische stellung von Rissen und Klüften in Slazgebirge. GSF Bericht T–200

Werner D, Doebl F (1974) Eine geothermische Karte des Rheingrabenuntergrundes, No. 8

Wilkins RWT, Bird JR (1980) The use of proton irradiation to reveal growth and deformation features in fluorite. Am Mineral 65:374–380